Regeneration of Three-Disulfide Mutants of Bovine Pancreatic Ribonuclease A Missing the 65−72 Disulfide Bond: Characterization of a Minor Folding Pathway of Ribonuclease A and Kinetic Roles of Cys65 and Cys72[†]

Michio Iwaoka,[‡] Darmawi Juminaga, and Harold A. Scheraga*

Baker Laboratory of Chemistry, Cornell University, Ithaca, New York 14853-1301

Received October 13, 1997; Revised Manuscript Received January 29, 1998

ABSTRACT: The oxidative regeneration pathways of two three-disulfide mutants of bovine pancreatic ribonuclease A (RNase A) missing the 65−72 disulfide bond, [C65S,C72S] and [C65A,C72A], have been studied by using oxidized dithiothreitol (DTT^{ox}) as an oxidizing agent and 2-aminoethylmethanethiosulfonate (AEMTS) as a thiol-blocking agent at 25 °C and pH 8.0. These mutants are analogues of the des-[65−72] intermediate, which is one of the two major three-disulfide intermediates that follow after the transition states in the regeneration pathways of wild-type RNase A [Rothwarf, D. M., Li, Y.-J., and Scheraga, H. A. (1998) *Biochemistry 37,* 3760−3766, 3767−3776.]. Both mutants folded through the same pathway but at a rate lower than that of the wild-type protein. The major rate-determining step in the regeneration of these mutants was determined to be the oxidation from the two-disulfide intermediates (2S) to the post-transition-state three-disulfide intermediate (3S*), suggesting the existence of a minor oxidation pathway (2S → 3S*, where 3S* is des-[65−72]) in the regeneration of the wild-type protein, in addition to one of the two major disulfide-rearrangement pathways (3S → des-[65−72]). The regeneration intermediates of these mutants (R, 1S, 2S, and 3S) participate in a steady state with a kinetic behavior resembling that of the wild-type protein. However, the apparent equilibrium constants (K_{eq}^{av}) in the steady state, averaged with statistical factors for these mutants, are significantly smaller than those for the wild-type protein, indicating that the intermediates in the regeneration of the mutants are relatively less stable by 0.32 kcal/mol. This difference is due to the decrease in the average rate constants for intramolecular disulfide-bond formation (k_{intra}^{av}) for the mutant proteins. Loop entropy calculations indicate that the increase in the average length of all possible disulfide loops of the mutants due to the replacement of Cys65 and Cys72 is not sufficient to account for the observed reduction of the values of k_{intra}^{av} for the mutants. Therefore, it is the removal of energetic factors (arising from the loss of the 65−72 disulfide loop) that leads to deceleration of the regeneration of the mutant proteins. The formation of the 65−72 disulfide loop in the regeneration of wild-type RNase A appears to facilitate the subsequent folding events.

Predicting the folded structure of a protein molecule from its amino acid sequence in terms of interresidue interactions is a goal of current protein folding studies. To accomplish this, it is necessary to characterize the conformations and energetic properties of intermediates in the folding pathways. When folding is coupled to disulfide-bond formation, information about folding is provided directly by isolation and identification of all disulfide-bonded intermediates in the regeneration pathways. However, this information is usually not easy to obtain, even though appropriate regeneration conditions and suitable methods for analyzing isolated intermediates are employed, primarily because of the number of possible disulfide-bonded intermediates.

Bovine pancreatic ribonuclease A (RNase A)[1] is a typical monomeric protein, consisting of 124 amino acid residues and four internal disulfide bonds (26−84, 40−95, 58−110, and 65−72). This small protein has attracted continuous interest since the landmark discovery by Anfinsen (*1*) that the protein contains all the necessary structural information in its amino acid sequence. Many different experiments have been designed to obtain information about the folding pathways of RNase A (*2*−*10*). Recent studies in our

[†] This work was supported by Research Grant GM-24893 from the National Institute of General Medical Sciences of the National Institutes of Health.

* To whom correspondence should be addressed.

[‡] Visiting scientist from the University of Tokyo.

[1] Abbreviations: RNase A, bovine pancreatic ribonuclease A; DTT^{ox}, oxidized dithiothreitol; DTT^{red}, DL-dithiothreitol; AEMTS, 2-aminoethylmethanethiosulfonate [$(NH_2)C_2H_4SSO_2CH_3$]; des-[65−72], wild-type RNase A in which the 65−72 disulfide bond is reduced; des-[40−95], wild-type RNase A in which the 40−95 disulfide bond is reduced; HPLC, high-performance liquid chromatography; NMR, nuclear magnetic resonance; [C65S,C72S] and [C65A,C72A], the three-disulfide mutants of RNase A in which cysteines 65 and 72 have been replaced by serines and alanines, respectively; [C40A,C95A], the three disulfide mutant of RNase A in which cysteines 40 and 95 have been replaced by alanines; RP-HPLC, reverse-phase high-performance liquid chromatography; MALDI−TOF, matrix assisted laser desorption ionization−time-of-flight; Tris, tris(hydroxymethyl)aminomethane; EDTA, ethylenediaminetetraacetic acid; GdnSCN, guanidine thiocyanate; HEPES, 4-(2-hydroxyethyl)-1-piperazineethanesulfonic acid; BPTI, bovine pancreatic trypsin inhibitor.

S0006-2960(97)02532-4 CCC: $15.00
Published on Web 03/12/1998

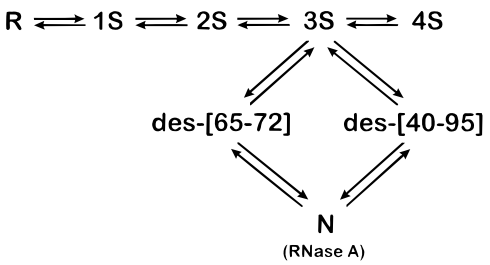

FIGURE 1: Regeneration pathways of RNase A at pH 8.0, 25 °C. DTT^{ox} and DTT^{red} are used as the redox couple (*13a*). R, 1S, 2S, 3S, and 4S are ensembles of molecules with the corresponding number of disulfide bonds, and N is the native protein.

laboratory involve DTT^{ox}/DTT^{red}-coupled regeneration experiments using AEMTS as a thiol-blocking agent (*11*−*13*) and the use of mutant proteins (*14*, *15*). A study of the folding properties of mutants is of interest because it helps to identify the roles of the substituted amino acids in the folding of the wild-type protein, by comparing the results for the mutants and the wild-type protein obtained under similar conditions.

In earlier studies of the regeneration of RNase A from the totally reduced form (R) to the folded native state (N), there was a controversy about the nature of the rate-determining step in the folding pathway; Creighton et al. proposed that only a single pathway exists (*8*, *16*), whereas Konishi et al. proposed the existence of multiple folding pathways with different rate-determining steps for each pathway depending on the solution conditions (*7b*, *17*). However, recent further extensive studies of the regeneration of RNase A (*12*, *13*) have unambiguously confirmed that RNase A regenerates through parallel multiple folding pathways. In these studies, DTT^{ox}/DTT^{red} and AEMTS were used as a redox couple and a thiol-blocking agent, respectively, and the main regeneration pathways and two post-transition-state intermediates denoted as des-[65−72] and des-[40−95] have been characterized (Figure 1).

The use of the cyclic DTT^{ox} has an advantage over the use of linear disulfides such as oxidized glutathione because mixed-disulfide intermediates between the protein and the oxidizing agent are not normally well populated in the regeneration solution. With mixed-disulfide intermediates, the number of possible disulfide-bonded intermediates in the case of four-disulfide proteins such as RNase A is 7193, including the totally reduced species (R). This is much larger than the number of the possible internal disulfide-bonded intermediates (763 possible species). The use of AEMTS is also important. The reaction of AEMTS with a free thiol is at least 5 orders of magnitude faster than that of traditional blocking agents such as iodoacetate (*11*), thereby reducing the possibility of thiol−disulfide exchange during the blocking process. In addition, blocking by AEMTS introduces one unit of positive charge into the regeneration intermediates, so that they can be separated in the subsequent HPLC analysis on the basis of the number of the cysteines blocked by AEMTS. Thus, the use of proper experimental conditions simplifies the resulting kinetic data and facilitates a more accurate deduction of the folding pathways. However, it should be kept in mind that the major regeneration pathways can shift from one to another depending on the regeneration conditions (*12*, *18*).

In the major regeneration pathways of RNase A at pH 8.0, 25 °C, all pre-transition-state intermediates (R, 1S, 2S, 3S, 4S) are structurally disordered and achieve a steady state after a certain regeneration time (*12*). The rate-determining steps are the disulfide rearrangements from 3S to the des-[65−72] and des-[40−95] intermediates (*13*). While 1S, 2S, 3S, and 4S are ensembles of many intermediates with a different number of internal disulfide bonds, des-[65−72] and des-[40−95] are unique post-transition-state intermediates that appear after the rate-determining step and fold rapidly to the native state (N) (*13*). Recent NMR studies of the three-disulfide RNase A mutants, [C65S,C72S] (*19*) and [C40A,C95A] (*20*), which are structural analogues of des-[65−72] and des-[40−95], respectively, have suggested that des-[65−72] and des-[40−95] have three-dimensional folded structures that are similar to that of the native state (N) of RNase A but are globally less stable with substantial fluctuation in the mutated disulfide loop and in its neighborhood. Therefore, in the rate-determining step of the major regeneration pathways (3S → des-[65−72] and des-[40−95]), both disulfide rearrangement and conformational folding are involved.

In this paper, the regeneration pathways of [C65S,C72S] and [C65A,C72A], analogues of the des-[65−72] intermediate, are determined under the same regeneration conditions as used for wild-type RNase A (pH 8.0, 25 °C, using DTT^{ox}/DTT^{red} as the redox couple and AEMTS as the thiol-blocking agent). Since these mutants have only six cysteines, direct disulfide rearrangement of misfolded 3S intermediates cannot occur, implying that regeneration of these mutants cannot proceed by rearrangement from 3S to the native species (N) with three native disulfide bonds but must follow a different chemical process as a rate-determining step. This different pathway can also be utilized for regeneration of the wild-type des-[65−72] intermediate, because similar disulfide-bonded intermediates may be involved in regeneration of both the mutants and the wild-type protein. In the case of the wild-type protein, misfolded 3S intermediates still have two free thiols, and it has been shown that disulfide rearrangement from 3S to the des-[65−72] and des-[40−95] intermediates constitutes the main regeneration pathways (*13*). Therefore, a study of the regeneration pathway of the mutants will reveal an alternative pathway toward des-[65−72] for the wild-type protein, in addition to the main rearrangement pathway, 3S→des-[65−72]. The elucidation of this alternative regeneration pathway of RNase A is one of the main goals of this paper.

Another aspect of the present regeneration study using these mutants concerns the proposal that the 65−72 disulfide loop is located in one of the chain folding initiation sites (CFIS) of RNase A (*21*, *22*). A CFIS is a specific region of a polypeptide chain that folds fast at the beginning and plays an important role in the early folding processes by limiting the conformational space (*21*, *23*). The importance of the 65−72 disulfide loop as a CFIS has recently been demonstrated by a quantitative analysis of the components of the 1S ensemble isolated in the regeneration of wild-type RNase A, showing that the one-disulfide intermediate that has the 65−72 disulfide linkage constitutes 40% of all the possible 28 1S-intermediates (*22*). This population is 2.4 times larger than the random distribution expected from loop entropy calculations. Therefore, there are enthalpic factors that stabilize the 65−72 disulfide loop in the early regeneration intermediates. [C65S,C72S] and [C65A,C72A] mutants

cannot form the stable 65−72 loop during the regeneration processes because they lack Cys65 and Cys72. Therefore, if the 65−72 loop is a real CFIS of RNase A, the regeneration processes of these mutants should be significantly slower than those of the wild-type protein. There is also an intrinsic change of disulfide loop entropy caused by the mutation of the two cysteines (Cys65 and Cys72); these cysteines are located in the middle of the polypeptide chain and can lead to the formation of small disulfide loops, which are entropically more stable than larger ones, during the regeneration of the wild-type protein. The loss of these cysteines in the mutants, therefore, destabilizes all regeneration intermediates of the mutants entropically so as to slow the regeneration processes. Considering both these enthalpic and entropic effects involving the 65−72 disulfide loop, the kinetic properties of the mutants will be compared with those of wild-type RNase A, and the kinetic roles of Cys65 and Cys72 in the regeneration of RNase A will be discussed.

MATERIALS AND METHODS

Materials. RNase A (type 1-A, Sigma Chemical Co.) was purified as described previously (*12a*). DTT^{red} ultrapure was obtained from Boehringer-Mannheim and used without further purification. DTT^{ox} (Sigma, Chemical Co.) was purified by the method of Creighton (*5b*). Since the DTT^{ox} obtained by this method still contained a small amount of impurities [∼0.03% as revealed by thiol analysis with Ellman's reagent (*24*, *25*) and by RP-HPLC with a Waters C-18 column], the DTT^{ox} was purified further by recrystallization from absolute ethanol; this procedure yielded pure DTT^{ox} with >99.999% purity as determined by RP-HPLC and with a recovery of 62%. AEMTS was synthesized as described by Bruice and Kenyon (*26*). All other reagents were of the highest grade commercially available and used without further purification.

Preparation of [C65S,C72S] and [C65A,C72A] Mutants. The [C65S,C72S] and [C65A, C72A] mutants were prepared, expressed, and purified by the procedures described by Laity et al. (*20*, *27*) and Shimotakahara et al. (*19*). The vectors were constructed by subcloning the [C65S/A,C72S/A] RNase A gene from pSJII[C65S/A,C72S/A] into the *Msc*I/*Hin*dIII region of a pET22b vector (Novagen) according to the procedure of delCardayré et al. (*28*). The *Msc*I site was created by the polymerase chain reaction (PCR) using a Perkin-Elmer Gene Amp PCR System 2400. The purity of the resulting mutant proteins was confirmed by cation-exchange HPLC, and their identities were confirmed by amino acid analysis and MALDI−TOF mass spectrometry.

Regeneration of [C65S,C72S] and [C65A,C72A]. Regeneration experiments were carried out following the method reported by Rothwarf and Scheraga (*12a*). The [C65S,C72S] or [C65A,C72A] mutant (0.5−1.0 mM) was reduced with a 100-fold molar excess of DTT^{red} in a pH 8.0 buffer containing 100 mM Tris, 2 mM EDTA, and 4 M GdnSCN for 2−3 h at 25 °C. The solution of the reduced protein was then buffer-exchanged into 100 mM Tris/2 mM EDTA, pH 8.0, using an HR 10/10 column packed with Sephadex G25 resin under continuous purging with argon at 25 °C. The time between the loading onto the column and the initiation of the regeneration process was less than 20 min. The concentration of the reduced protein in the collected eluent was determined with Ellman's reagent (*24*) using $\epsilon = 13\,900\ M^{-1}\ cm^{-1}$ at 412 nm (*25*).

The regeneration process was initiated by adding the reduced protein solution into a solution of 100 mM Tris/2 mM EDTA, pH 8.0, containing the desired amount of oxidized DTT under argon. The concentration of the reduced protein ranged from 1.3 to 23 μM for the [C65S,C72S] mutant (six different concentrations) and from 3.3 to 44 μM for the [C65A,C72A] mutant (eight different concentrations); the concentration of DTT^{ox} ranged from 34 to 185 mM. The concentration of DTT^{red} was always zero in the beginning but increased as the regeneration proceeded. All experiments were carried out at 25 °C. The reaction temperature was regulated within ±0.1 °C by using an insulated jacketed outer vessel connected to a Fisher Scientific Model 9100 refrigerated circulating bath. The regeneration mixture was maintained under a continuous flow of humidified argon in order to avoid air oxidation. The total concentration of thiol was checked for all reaction mixtures at the end of the regeneration experiment by Ellman's analysis (*24*). The loss of thiol due to air oxidation was estimated to be less than 5%.

After selected time intervals, aliquots (usually 0.6 mL) were collected from the regeneration mixture, and unreacted thiols were blocked by the addition of ∼100-fold excess of AEMTS dissolved in 0.1 mL of 100 mM Tris/2 mM EDTA, pH 8.0. The blocking reaction results in the rapid conversion of all thiols in the sample to mixed disulfides with cysteamine (2-aminoethanethiol) (*11*, *12a*, *26*). After 5 min, the pH of the sample was reduced below 5 by adding 5 μL of acetic acid to facilitate subsequent chromatographic analysis and to avoid deamidation during storage. The sample solution was stored frozen at −20 °C until the HPLC fractionation was carried out.

Fractionation and Identification of Intermediates. The HPLC system consists of a model SP8700 pump system from Spectra Physics equipped with a Hydropore SCX 5 μm cartridge column from Rainin. The detector was an ISCO UA-5 with a type 9 optical unit and a 280 nm filter. A ternary gradient was used. Buffer A contained 25 mM HEPES and 1 mM EDTA, pH 7.0. Buffer B contained 25 mM HEPES, 1 mM EDTA, and 1 M NaCl, pH 7.0. Buffer C contained 50 mM acetic acid and 1 mM EDTA, pH 5.0. The sample solution that was diluted with buffer C was injected on to the column equilibrated with buffer C. After changing the eluting buffer to buffer A (in 5 min), the system was equilibrated with 95% buffer A and 5% buffer B for 7 min. Then, an NaCl gradient was applied by changing the ratio of buffer B from 5% to 20% in 60 min (at 0 °C) to elute the regeneration intermediates separately. The folding intermediates emerged from the cation exchange column as groups (N, 3S, 2S, 1S, and R) depending on their net charge, which was modified by cysteamines introduced in the intermediates by blocking of the free thiol groups with AEMTS. Figure 2 shows representative chromatograms as a function of regeneration time for [C65S,C72S]. Similarly, Figure 3 shows representative chromatograms as a function of regeneration time for [C65A,C72A].

To identify the number of disulfide bonds in the intermediates separated by the HPLC, a postcolumn disulfide-detection analysis (*29*) was employed. The analysis is quantitative for the relative number of disulfide bonds in a molecule; thus, we could determine the number of disulfide

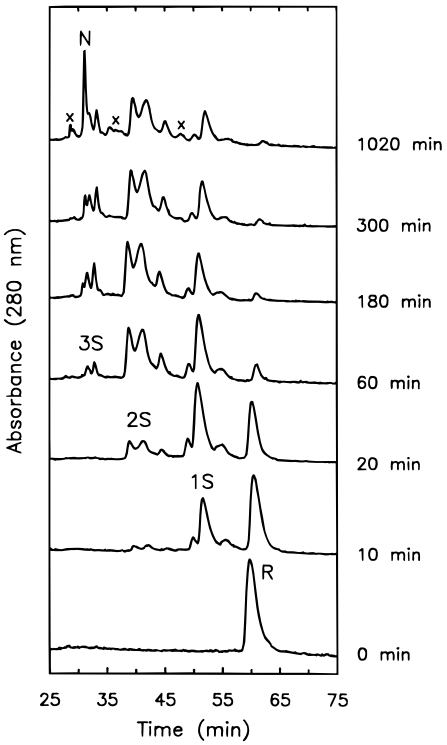

FIGURE 2: Series of chromatograms for the regeneration of [C65S, C72S] showing the appearance of intermediates with time. Starting regeneration conditions were 8.2 μM [C65S,C72S], 162 mM DTT^{ox}, pH 8.0, and 25 °C. The peaks marked by X were assigned to deamidated intermediates.

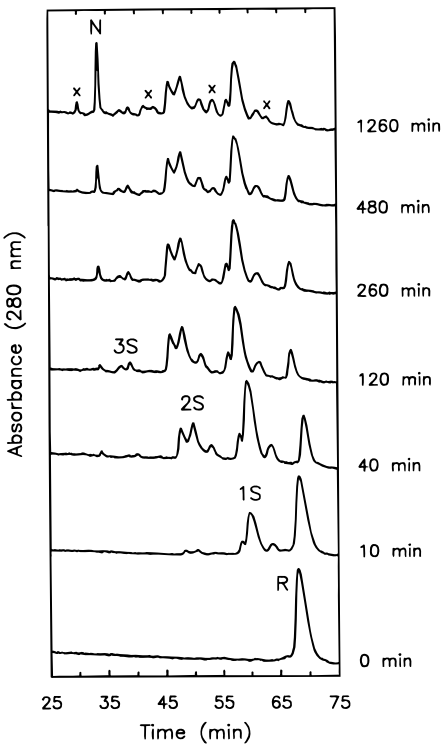

FIGURE 3: Series of chromatograms for the regeneration of [C65A, C72A] showing the appearance of intermediates with time. Starting regeneration conditions were 18 μM [C65A,C72A], 133 mM DTT^{ox}, pH 8.0, and 25 °C. The peaks marked by X were assigned to deamidated intermediates.

bonds in each intermediate. By using the folded native species (N) or the totally reduced one (R) blocked by AEMTS as an internal standard, we assigned the peaks having three disulfide bonds in a molecule to the 3S intermediate, the peaks having four-disulfide bonds to 2S (two intramolecular SS bonds and two mixed SS bonds with cysteamine), and the peaks having five-disulfide bonds to 1S (one intramolecular SS bond and four mixed SS bonds with cysteamine).

Furthermore, we measured the MALDI−TOF mass spectra using the Finniganmat Lasermat model 2000 mass spectrometer for each group of intermediates, which were AEMTS-blocked, fractionated by using the same HPLC system, and desalted with an Amicon YM3 membrane. The matrix used was α-cyano-4-hydroxycinnamic acid. The mass number was calibrated by using wild-type RNase A as an external standard. Although it is known that disulfide bonds may possibly be broken during the MALDI−TOF measurement (*18*, *30*), we observed only one major peak for a particular group of intermediates. The mass numbers at the center of the major peak for each intermediate in the case of [C65S,C72S] were 13 655 (13 653) for N, 13 661 (13 653) for 3S, 13 820 (13 807) for 2S, 13 960 (13 961) for 1S, and 14 098 (14 115) for R; while in the case of [C65A,C72A] they were 13 626 (13 621) for N, 13 624 (13 621) for 3S, 13 784 (13 775) for 2S, 13 905 (13 929) for 1S, and 14 082 (14 083) for R; the values in parentheses represent the calculated mass numbers for each AEMTS-blocked intermediate. These data unambiguously confirmed the assignments of the 1S, 2S, and 3S intermediates by the postcolumn disulfide-detection analysis. It should be noted that the fraction of N was homogeneous in these mass measurements, eliminating the possibility that this fraction contained impurities, such as 2S and the mixed intermediates with DTT^{red}. Another possibility that this fraction might contain misfolded 3S is very low because N and 3S could be well separated by cation-exchange HPLC (as shown in Figure 3) and also because the profile of 3S in the early stages of regeneration did not involve a significant peak at the elution time of N (as shown in Figure 2).

Kinetic Analysis. Because the postcolumn disulfide-detection analysis is quantitative for the number of disulfide bonds (*29*), it allowed us to calculate the relative molar amounts of each intermediate group in the AEMTS-blocked regeneration mixture, which are necessary for the later kinetic analysis. It is known that the molar extinction coefficients of each folding intermediate at a specific wavelength (280 nm in this paper) vary slightly from R to N as shown recently by Thannhauser et al. (*18*). By comparing the results of the quantitative disulfide-detection system with that of a UV chromatogram of the same sample, we obtained the relative molar extinction coefficients of each intermediate with respect to R. The relative molar extinction coefficients obtained by this method were 1.18 (N), 1.13 (3S), 1.02 (2S), 1.00 (1S), and 1.00 (R) for [C65S,C72S] and 1.22 (N), 1.05 (3S), 1.00 (2S), 1.01 (1S), and 1.00 (R) for [C65A,C72A] with an error less than ±5%. By using these values, the relative amounts of each intermediate were simply determined from the UV chromatograms.

The kinetic data, which were obtained by the HPLC analysis and corrected for the relative molar extinction coefficients as described above, were interpreted by the general KOS (Konishi−Ooi−Scheraga) approach (*7b*) to determine the major rate-determining step. Using this approach for a three-disulfide mutant, there are 10 possible rate-determining steps (*18*); this will be described in the

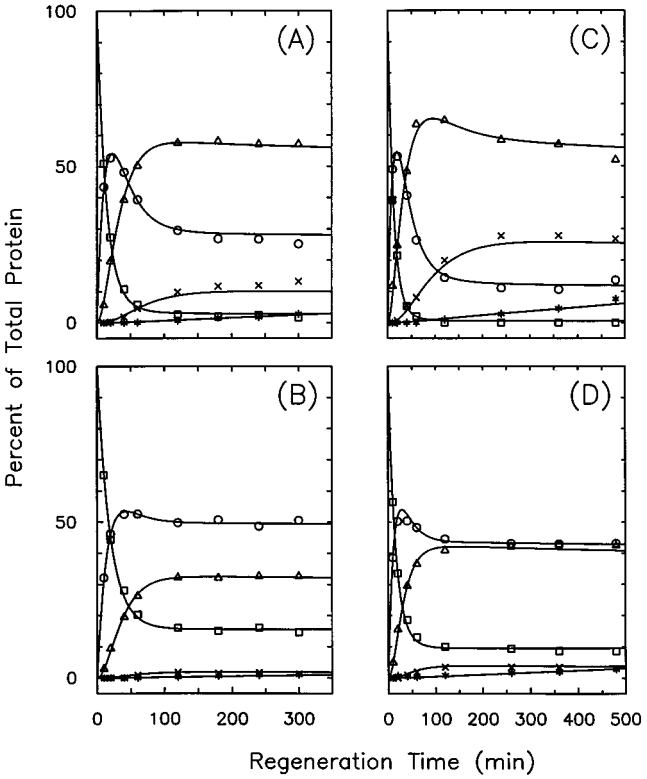

FIGURE 4: Concentration of native protein and the intermediates as a function of regeneration time at pH 8.0 and 25 °C. (□) Reduced protein; (○) one-disulfides; (△) two-disulfides; (×) three-disulfides; (*) folded native mutant. The starting concentrations were as follows: (A) 8.2 μM [C65S,C72S] and 162 mM DTT^{ox}, (B) 23 μM [C65S,C72S] and 99 mM DTT^{ox}, (C) 3.4 μM [C65A,C72A] and 185 mM DTT^{ox}, and (D) 18 μM [C65A,C72A] and 133 mM DTT^{ox}. The symbols represent the experimental data; the curves are drawn using the rate constants given in Tables 2 and 3.

Results section. Since deamidation occurred at significant rates in the regeneration experiments of the mutants, ~15% in 20 h for the [C65S,C72S] mutant and ~10% in 20 h for the [C65A,C72A] mutant, only data collected up to 300 and 480 min, respectively, were employed in the kinetic analysis. Within these time limits, the amounts of deamidated proteins were estimated to be less than 4%. The kinetic data were analyzed by two methods. In the first, the dependence of the rate of formation of N on the concentrations of different intermediates and of DTT^{ox} and DTT^{red} was analyzed by graphical fitting to determine the rate equation for formation of N in the steady state. In the second, a modified simplex minimization procedure was employed to fit all data sets simultaneously (*12b*, *31*). Error estimates were determined by a Monte Carlo procedure (*32*) and are given at the 95% confidence limit. Figure 4 shows the representative time-dependence behavior for the relative populations of the native protein and the intermediates; the symbols represent the experimental data, and the solid lines represent the calculated curves using the rate constants determined by the full computational (modified simplex minimization procedure) fitting. Figure 4 demonstrates that, in general, the intermediates achieve a steady state within ~120 min. After this time, a slight change due to the generation of the native protein can be seen.

Deamidation. In the HPLC chromatograms of the regeneration mixtures, we found small peaks (× in Figures 2 and 3) in front of every major peak. We assigned these as deamidated byproducts for the following reasons. First, these minor species elute earlier than their corresponding major species, which means that these species have lower positive charge; deamidation replaces an asparagine with an aspartic acid (*33*) that is ionized at the pH of the HPLC eluent (pH 7.0). Second, the elution times of these species (×) are consistent with those deamidation peaks of the wild-type protein which has been well studied (*29*).

Table 1: Equilibrium Constants at 25 °C and pH 8.0

	[C65S,C72S]		[C65A,C72A]		wt RNase A
reaction	K_{eq}^{obs}[a] ($\times 10^4$)	K_{eq}^{av}[b] ($\times 10^4$)	K_{eq}^{obs}[a] ($\times 10^4$)	K_{eq}^{av}[b] ($\times 10^4$)	K_{eq}^{av}[c] ($\times 10^4$)
R ↔ 1S	8.8 ± 0.9	0.59	8.7 ± 0.6	0.58	1.0
1S ↔ 2S	1.7 ± 0.2	0.57	1.9 ± 0.2	0.62	0.89
2S ↔ 3S	0.16 ± 0.03	0.50	0.17 ± 0.02	0.56	0.98
(3S ↔ 4S)					0.88

[a] This dimensionless equilibrium constant was calculated as an average over all experiments in which steady-state concentrations of the individual species were determined (see eqs 1−3). [b] K_{eq}^{av} is K_{eq}^{obs} corrected for statistical factors as described in the text. [c] The data are calculated from the values of k_f^{av} and k_r^{av} reported by Rothwarf et al. (*13b*).

RESULTS

Steady State and Equilibrium Constants. From Figures 2−4, it can be seen that, within 120 min after the regeneration is initiated, the system approaches a steady state in which the relative concentration of each intermediate remains constant while the amount of N is slowly increasing. Starting from different initial concentrations of the mutant proteins and DTT^{ox}, a steady state was also achieved; however, the relative population of each regeneration intermediate was different depending on the initial conditions. A similar behavior was also observed in the oxidative regeneration of wild-type RNase A (*12a*). The apparent equilibrium constants were calculated from all experimental data for the steady states attained under different initial conditions according to the following equations:

$$R + DTT^{ox} \overset{K_1}{\rightleftharpoons} 1S + DTT^{red} \quad (1)$$

$$1S + DTT^{ox} \overset{K_2}{\rightleftharpoons} 2S + DTT^{red} \quad (2)$$

$$2S + DTT^{ox} \overset{K_3}{\rightleftharpoons} 3S + DTT^{red} \quad (3)$$

where 3S does not include N. The concentrations of DTT^{ox} and DTT^{red} at each regeneration time were obtained according to eqs 4 and 5:

$$[DTT^{ox}] = [DTT^{ox}]_{initial} - [DTT^{red}] \quad (4)$$

$$[DTT^{red}] = [1S] + 2[2S] + 3([3S] + [N]) \quad (5)$$

The resulting values of the equilibrium constants (K^{obs}) are presented in Table 1.

Since the 1S, 2S, and 3S intermediates are ensembles of many individual species as seen in Figures 2 and 3, the observed apparent equilibrium constants (K^{obs}) do not have any important physical meaning. To compare the values of K^{obs} of the three-disulfide mutants to those of the wild-type protein obtained under the same regeneration conditions, average apparent equilibrium constants (K^{av}) were calculated

by considering statistical factors; for example, there are 15 possible intermediates in the 1S grouping, 45 possible intermediates in the 2S grouping, and 14 possible intermediates in the 3S grouping (which is assumed not to include N). Therefore, K_1, K_2, and K_3 were divided by factors of 15, 3 (= 45/15), and 0.31 (= 14/45), respectively, to obtain the values of K^{av} listed in Table 1. These values represent limits of the average equilibrium constants, which depend on how the distribution of regeneration intermediates is populated.

The resulting values of K^{av} are approximately constant ($\sim 0.57 \times 10^{-4}$), independent of the process involved. This clearly indicates that the average free energies for the oxidation states (R, 1S, 2S, and 3S in the presence of DTT^{ox} and DTT^{red}) are equally separated ($\Delta G° = 5.8$ kcal/mol) from each other; neither one is more stabilized than the other. A similar behavior was also observed for wild-type RNase A as shown in Table 1 (*13b*). However, the values of K^{av} for the mutants and wild-type RNase A are different as will be discussed in the Discussion section.

Another important property of the steady state is that the profiles of the peaks of the intermediate groupings (1S, 2S, 3S) in the HPLC chromatograms do not change with reaction conditions and regeneration time. Since these peak profiles reflect the populations of the individual intermediates that are involved in each grouping, intramolecular disulfide rearrangements within the disulfide grouping are much faster than the oxidation and reduction rates of the intermediates in the steady state; estimates of the rearrangement rates will be given in the Discussion section.

Rate-Determining Steps. According to the KOS approach (*7b*), all possibilities should be considered for the rate-determining steps from the preequilibrated intermediates to the post-transition-state intermediates. In the case of a three-disulfide mutant such as [C65S,C72S] or [C65A,C72A], there are 10 possible rate-determining steps; as discussed in detail recently by Thannhauser et al. (*18*), these are R→1S*, 1S→2S*, 2S→3S*, 1S→R*, 2S→1S*, 3S→2S*, R→R*, 1S→1S*, 2S→2S*, and 3S→3S*. The intermediates marked by an asterisk are those that appear in the rate-determining step and fold quickly to the native state (N). These 10 possible rate-determining steps can be categorized in three types of reactions: an oxidation with DTT^{ox}; a reduction with DTT^{red}; and a unimolecular rearrangement that may involve unimolecular disulfide-bond reshuffling and conformational rearrangement. If the rate-determining step of the major regeneration pathway involves only an oxidation (or reduction) step, then the rate of regeneration of the native state (N) should depend on the concentrations of both the specific intermediate and DTT^{ox} (or DTT^{red}). By contrast, if the rate-determining step of the major folding pathway involves a rearrangement process, the rate of regeneration of N does not depend on the concentration of DTT^{ox}/DTT^{red} but depends only on the concentration of the specific intermediate.

Figure 5 shows the time dependence of the regenerated amount of N for the [C65A,C72A] mutant under different initial conditions. The symbols represent experimental data, and the lines represent the theoretical curves drawn using the final regeneration model and rate constants. From this figure, it is clear that there is a time delay (~20 min) before N begins to regenerate. This suggests that N does not

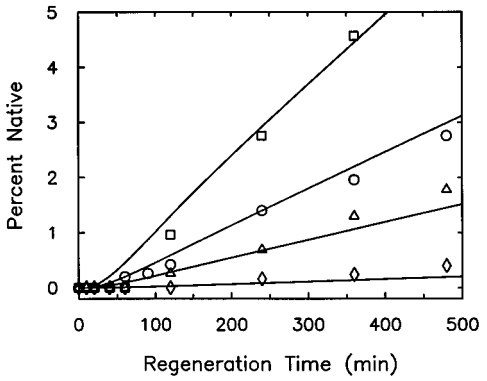

FIGURE 5: Plot of the appearance of native [C65A,C72A] as a function of regeneration time, at pH 8.0 and 25 °C. The symbols represent the experimental data; the curves were generated by using the rate constants given in Tables 2 and 3. The starting conditions were (□) 3.4 μM [C65A,C72A] and 185 mM DTT^{ox}, (○) 18 μM [C65A,C72A] and 133 mM DTT^{ox}, (△) 31 μM [C65A,C72A] and 100 mM DTT^{ox}, and (◇) 36 μM [C65A,C72A] and 34 mM DTT^{ox}.

regenerate from the early populated intermediates such as R and 1S. Therefore, the major rate-determining step may not originate from the R and 1S intermediates. Once the steady state has been achieved (~120 min), the concentration of each intermediate and the concentrations of DTT^{ox} and DTT^{red} remain approximately constant; more precisely, the concentration of DTT^{red} changes slowly as the regeneration of N proceeds, but the change is not significant so that the steady state will not be altered (*12a*, *b*, *18*). Therefore, it can be seen that the rate of formation of N is almost constant after the steady state is achieved. Subsequently, we calculated the rate of formation of N and the concentrations of R, 1S, 2S, 3S, DTT^{ox}, and DTT^{red} in the steady state and fitted them to every model for the 10 possible rate-determining steps. According to this graphical fitting, we found that there are two candidates for the major rate-determining step; these are the oxidation process 2S→3S*, with the rate equation $d[N]/dt \propto [2S][DTT^{ox}]$, and the reduction process 3S→2S*, with the rate equation $d[N]/dt \propto [3S][DTT^{red}]$. With the information presented thus far, these two processes are indistinguishable because the terms in their rate equations, $[2S][DTT^{ox}]$ and $[3S][DTT^{red}]$, are related by the equilibrium constant, K_3, in the steady state (eq 3). The same analysis was carried out for the [C65S,C72S] mutant (data not shown), and the same result was obtained.

A full computational (modified simplex minimization procedure) fitting was also employed to determine the major rate-determining step. In this procedure, seven rate constants were considered: six are for the equilibria between R and 1S, 1S and 2S, and 2S and 3S; the seventh is for one of the 10 possible rate-determining steps. We applied every possible model for a rate-determining step to fit the experimental data and calculated the final fitting parameters by a least-squares method. With the oxidation process, 2S→3S*, as the rate-determining step, the best fit [based upon the residual values of χ^2 (data not shown)] was obtained for regeneration of both [C65S,C72S] and [C65A,C72A]. This result is consistent with that obtained from the graphical fitting analysis of the [N] vs time plot, i.e., [N] is linear in t ($d[N]/dt$ is constant) because k, $[DTT^{ox}]$, and [2S] are essentially constant. However, the 3S→2S* process did not yield as good a fit in the full computational fitting. Therefore, in contrast to the graphical fitting described above,

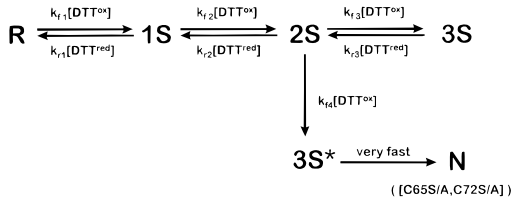

FIGURE 6: Final regeneration model of [C65S/A,C72S/A]; rate constants are given in Tables 2 and 3. The rate-determining step is the bimolecular oxidation process (k_{f4}) of 2S with DTT^{ox} to produce 3S* and DTT^{red}.

the computational method was able to single out 2S→3S* as the major rate-determining step. In the full computational fitting, the rearrangement process, 2S→2S*, gave the second best fit as a rate-determining step. It is possible that this 2S→2S* rearrangement is a minor rate-determining step in the regeneration of these mutants.

According to the above fittings, the final kinetic model that accounts for the regeneration of the mutants is presented in Figure 6. In this model, R, 1S, 2S, and 3S attain a pre-transition equilibrium, and the oxidation 2S→3S* is the rate-determining step. The conversion of 3S* to N is presumably a conformational rearrangement. Strictly speaking, the rate-determining step could be reversible. However, since the estimated rate of reduction of N to 2S [$k = 3.1 \times 10^{-2}$ min^{-1} M^{-1} (*31*)] should be a factor of 10^2 slower than that of the oxidation of 2S to 3S* (i.e., to N) ($k_{f4} \sim 1.0 \times 10^{-3}$ min^{-1} M^{-1}; Table 2) under the strong oxidizing conditions employed here ($[DTT^{red}]/[DTT^{ox}] < 0.001$), we ignored the reverse process of the rate-determining step in the kinetic analysis.

Rate Constants. According to the full computational fitting, we determined seven rate constants for the kinetic scheme (Figure 6). The results are given in Tables 2 and 3 along with the average values corrected for statistical factors, and the corresponding values obtained for wild-type RNase A from Rothwarf et al. (*13b*). The average rate constants were calculated as follows. For example, for the oxidation of R, there are 15 possible ways to form a disulfide bond from six free thiols. Therefore, k_{f1}^{obs} was divided by a factor of 15 to obtain the value of k_{f1}^{av}. Similarly, k_{f2}^{obs} and k_{f3}^{obs} were divided by factors of 6 and 1, respectively, to obtain the values of k_{f2}^{av} and k_{f3}^{av}. For the reduction of 3S, there are three possible ways to break one of three disulfide bonds. Therefore, k_{r3}^{obs} was divided by a factor of 3 to obtain the value of k_{r3}^{av}. Similarly, k_{r2}^{obs} and k_{r1}^{obs} were divided by factors of 2 and 1, respectively, to obtain the values of k_{r2}^{av} and k_{r1}^{av}. The rate constants for the two mutants were similar.

DISCUSSION

Similarity and Difference of the Two Mutants. The two residues, used to replace cysteines in [C65S,C72S] and [C65A,C72A] for the regeneration experiments, were selected because serine and alanine are regarded as good substitutes for cysteine in protein refolding studies (*34*, *35*). However, it is known that serine and alanine mutants frequently show somewhat different refolding properties (*14*, *36*) for reasons that are not clear. Therefore, for a general comparison of mutants and wild-type RNase A in disulfide-coupled regeneration processes, we compared the regeneration kinetics of [C65S,C72S] and [C65A,C72A]. The kinetic results for these two mutants were, however, similar to each other as shown in Tables 1−3 and Figures 2 and 3. The values of K_{eq} (Table 1), k_f (Table 2), and k_r (Table 3) were almost the same within experimental error, except that the values of k_{f1} and k_{f3} are slightly larger for [C65A,C72A] than for [C65S,C72S], suggesting that [C65A,C72A] regenerates slightly faster than [C65S,C72S]. However, this difference may not be significant in light of the overall similarities in the kinetic behaviors of these mutants. Moreover, the peak profiles of the regeneration intermediates (1S, 2S, and 3S) for [C65S,C72S] (Figure 2) and [C65A,C72A] (Figure 3) were very similar; the differences in the peak separation between N and 3S and also in the elution times of all intermediates are due to the use of a new cartridge column for HPLC analysis of the [C65A,C72A] mutant. The final regeneration pathways for [C65S,C72S] and [C65A,C72A] were also the same (Figure 6); they both achieved a steady state, and the rate-determining step on the main pathway was the oxidation from 2S to 3S*. These overall similarities indicate that serine and alanine have essentially the same effect as substitutes for cysteine in this case. Consequently, in the following discussion the results obtained for only [C65S,C72S] are considered.

However, Lester et al. (*14*) have recently studied the regeneration of two RNase A mutants, in which four cysteines (Cys40, Cys65, Cys72, and Cys95) were replaced by either four serines or four alanines, and found that the two-disulfide species with two native disulfide pairings (Cys26−Cys84 and Cys58−Cys110) are more populated for the serine mutant than for the alanine mutant at 4 °C, pH 8.1. That result suggested that serine is a better substitute for cysteine in these mutants. This is contrary to our conclusion for [C65S,C72S] and [C65A,C72A], in which only a 65−72 disulfide bond is missing. We suggest that the discrepancy observed for the double mutant (missing two disulfide bonds) arises from different local interactions of the substituted serines and alanines at positions 40 and 95 rather than those at positions 65 and 72.

A Minor Folding Pathway in the Regeneration of RNase A. The [C65S,C72S] mutant is an analogue of the des-[65−72] intermediate that lies on one of the major regeneration pathways of wild-type RNase A (see Figure 1). The only structural difference is that des-[65−72] has two free thiol groups at Cys65 and Cys72, which can lead to the formation of the final disulfide bond of native RNase A or to unimolecular disulfide rearrangements to the misfolded 3S species, while the [C65S,C72S] mutant does not have these functional groups. The similarity in conformation of these two proteins has been demonstrated by NMR measurements on the isolated des-[65−72] intermediate blocked by AEMTS (*37*) and on the [C65S,C72S] mutant (*19*). According to these studies, both proteins have a similar folded structure with substantial flexibility at the loop containing residues 65−72 and in its neighborhood. However, while these investigations have indicated that [C65S,C72S] and des-[65−72] are conformationally similar to the wild-type protein, they are thermodynamically less stable; this is reflected in the facts that the enzymatic activity and the T_m of [C65S, C72S] are lower than those of wild-type RNase A (*19*, *27*).

In the main regeneration pathways of RNase A, des-[65−72] appears mainly through disulfide-bond reshuffling of 3S, which requires another intramolecular thiol group. In the

Table 2: Forward Rate Constants[a] at 25 °C and pH 8.0

	[C65S,C72S]			[C65A,C72A]			wt RNase A	
reaction	k_f^{obs}[b] ($\times 10^2$) (min^{-1} M^{-1})	k_f^{av}[c] ($\times 10^2$) (min^{-1} M^{-1})	k_{intra}^{av}[d] (min^{-1})	k_f^{obs}[b] ($\times 10^2$) (min^{-1} M^{-1})	k_f^{av}[c] ($\times 10^2$) (min^{-1} M^{-1})	k_{intra}^{av}[d] (min^{-1})	k_f^{av}[e] ($\times 10^2$) (min^{-1} M^{-1})	k_{intra}^{av}[e] (min^{-1})
R → 1S	42.3 ± 0.03[f]	2.8	4.3	43.4 ± 0.02[f]	2.9	4.5	5.2	8.0
1S → 2S	16.9 ± 0.02	2.8	4.3	17.0 ± 0.02	2.8	4.4	5.0	7.7
2S → 3S	2.2 ± 0.1	2.2	3.4	2.5 ± 0.1	2.5	3.8	6.2	9.6
2S → 3S*	0.10[g] ± 0.01			0.12[g] ± 0.01				
(3S → 4S)							4.3	6.7

[a] These rate constants were determined from the data for the whole time course under several different experimental redox conditions. [b] k_f^{obs} is the observed rate constant for formation of a protein disulfide bond using DTT^{ox} for the reaction indicated. [c] k_f^{av} is k_f^{obs} corrected for statistical factors, as described in the text. [d] k_{intra}^{av} is the average rate constant for formation of an intramolecular protein disulfide bond, determined from k_f^{av} using eq 6. [e] These data are from Rothwarf et al. (*13b*). [f] The error is calculated at the 95% confidence limit. [g] The rate constant of the rate-determining step.

Table 3: Reverse Rate Constants[a] at 25 °C, pH 8.0

	[C65S,C72S]		[C65A,C72A]		wt RNase A
reaction	k_r^{obs}[b] ($\times 10^{-2}$) (min^{-1} M^{-1})	k_r^{av}[c] ($\times 10^{-2}$) (min^{-1} M^{-1})	k_r^{obs}[b] ($\times 10^{-2}$) (min^{-1} M^{-1})	k_r^{av}[c] ($\times 10^{-2}$) (min^{-1} M^{-1})	k_r^{av}[d] ($\times 10^{-2}$) (min^{-1} M^{-1})
R ← 1S	4.8 ± 0.1[e]	4.8	4.9 ± 0.1[e]	4.9	5.2
1S ← 2S	9.3 ± 0.2	4.7	9.1 ± 0.1	4.6	5.6
2S ← 3S	14 ± 1	4.7	14 ± 1	4.7	6.3
(3S ← 4S)					4.9

[a] These rate constants were determined from the data for the whole time course under several different experimental redox conditions. [b] k_r^{obs} is the observed rate constant for reduction of a protein disulfide bond using DTT^{red} for the reaction indicated. [c] k_r^{av} is k_r^{obs} corrected for statistical factors, as described in the text. [d] The data are from Rothwarf et al. (*13b*). [e] The error is calculated at the 95% confidence limit.

regeneration of [C65S,C72S], however, this reshuffling process cannot take place between the pre-transition-state 3S intermediates (misfolded 3S intermediates) and the native state of [C65S,C72S] since this mutant contains no intramolecular thiol group. Instead, as described in the Results section, [C65S,C72S] folds through the 2S→3S* process as a rate-determining step. The similar oxidation pathway, 2S→des-[65−72], therefore may also be present in the regeneration of the wild-type protein because the regenerated 2S intermediates of the wild-type protein may contain structurally similar disulfide-bonded intermediates to those of the mutants.

This alternative regeneration pathway, viz., 2S→des-[65−72] for the wild-type protein, is slow as compared to one of the two main disulfide-rearrangement pathways, viz., 3S→des-[65−72], for the following reason. First, the rate of the reshuffling process, 3S→des-[65−72], in the regeneration of the wild-type protein has been determined to be

$$V_1 = (2.1 \times 10^{-3})[3S]\ (M \cdot min^{-1})$$

where [3S] is the concentration of the 3S intermediates in the regeneration mixture (*13b*). If we use the rate constant k_{f4} of the mutant 2S→3S* (Figure 6 and Table 2) as the rate constant for the alternative pathway 2S→des-[65−72], then the rate of formation of des-[65−72] through this alternative pathway is equal to

$$V_2 = (1.0 \times 10^{-3})[DTT^{ox}][2S']\ (M \cdot min^{-1})$$

where $[DTT^{ox}]$ is the concentration of DTT^{ox} and [2S′] is the concentration of the 2S intermediates excluding the intermediates that contain either 65−72, 65−*x*, or 72−*x* disulfide bonds. Because the population of the 1S intermediates that contain either 65−72, 65−*x*, or 72−*x* disulfide bonds is 67% in the 1S grouping (*22*), we assume that the value of [2S′] may be less than 33% of [2S]. Considering that $[DTT^{ox}]$ is less than 0.2 M and that the ratio [2S]/[3S] is less than 5 in the steady state under normal regeneration conditions (*12a*), the ratio of the reaction rates for the two pathways is

$$V_2/V_1 < 0.48 \times 0.33[DTT^{ox}][2S]/[3S] < 0.16$$

and the fraction of des-[65−72] that regenerates from the 2S→des-[65−72] pathway is

$$V_2/(V_1 + V_2) < 0.16/(1 + 0.16) < 0.14$$

Thus, the population of des-[65−72] that regenerates directly from 2S is at most 14%.

According to the recent regeneration study by Rothwarf et al. (*13b*), native RNase A regenerates mainly through disulfide-rearrangement pathways (3S→3S*, where 3S* consists of des-[65−72] and des-[40−95]), and the relative population of the 3S→des-[65−72] pathway is only less than 20%. Therefore, the population of the observed minor 2S→des-[65−72] pathway should be less than 14% × 0.2 ≈ 3% in the regeneration of wild-type RNase A. This minor pathway would be difficult to observe in a regeneration study of the wild-type protein because of its low population but could be seen only in the experiments using the [C65S/A, C72S/A] mutants. Thus, it is clearly shown again that RNase A folds through multiple pathways. Another minor regeneration pathway, 2S→des-[40−95], has also been characterized recently by Xu and Scheraga (*15*).

Assuming that 3S* is formed from 2S species that have two native disulfide bonds (because 2S species with incorrect disulfide bonds will reshuffle rapidly before 2S converts to 3S*), there are three possibilities for the formation of 3S* with three native disulfide bonds. For example, one possibility is that the intermediate has 26−84 and 40−95

disulfide bonds and forms a 58−110 disulfide bond in the rate-determining step; similarly, the 26−84 or 40−95 disulfide bond could be formed in the rate-determining step. The experimental results presented here cannot decide which of these three is the major pathway, nor if more than one of these three pathways is possible.

In the reduction of wild-type RNase A, the reduction of des-[65−72]→2S has been characterized as one of the important steps in these pathways (*31*). Our results indicate that the pathway from des-[65−72] to 2S is not irreversible, although the oxidation 2S→des-[65−72] is a significantly minor process as shown by its small population in the regeneration pathways of wild-type RNase A.

Energetic Features of Folding Intermediates. Table 1 lists the observed apparent equilibrium constants between the regeneration intermediates in the steady state. Because the intermediates are considered as groups, it is meaningful to compare the values of only K_{eq}^{av}, which are corrected by statistical factors. The values of K_{eq}^{av} observed for [C65S, C72S] were almost constant ($\sim 0.55 \times 10^{-4}$), showing that the free energy of each pre-transition-state intermediate in the presence of DTT^{ox} and DTT^{red} increases ($\Delta G^\circ = 5.8$ kcal/mol) upon formation of an additional disulfide bond to the same extent in each step on the average. This similar behavior has also been observed for wild-type RNase A (*13b*) as shown in Table 1; the values of K_{eq}^{av} for the wild-type protein are approximately 1.0×10^{-4}. These properties reflect the fact that most pre-transition-state intermediates for the mutant and the wild-type protein are predominantly disordered. By contrast, the corresponding values for another three-disulfide mutant of RNase A, [C40A,C95A], have been found to vary from 0.52×10^{-4} to 1.7×10^{-4} (*15*). This difference may arise from the presence of local conformations in the pre-transition-state intermediates of the [C40A, C95A] mutant, most likely around the disulfide bond 65−72 that are not present in [C65S,C72S]. The effect of these local structures may not be significant in the regeneration intermediates of wild-type RNase A because the number of possible disulfide-bonded intermediates for the wild-type protein (763 species) is much larger than for [C40A,C95A] (75 species).

The values of K_{eq}^{av} for [C65S,C72S], however, are distinctly smaller than those for wild-type RNase A, indicating that the regeneration intermediates of the mutant are relatively less stable than those of the wild-type protein. The destabilization energy is estimated to be 0.32 kcal/mol per formation of one disulfide bond, as calculated by using the average values of K_{eq}^{av}, viz., 0.55×10^{-4} for [C65S,C72S] and 0.94×10^{-4} for wild-type RNase A.

Theoretically, K_{eq}^{av} can be expressed as the ratio of the rate constants for the two half-reactions of the equilibrium (k_f^{av}/k_r^{av}). As shown in Tables 2 and 3, the values of k_f^{av} of the mutant are about a factor of 2 smaller than those of the wild-type protein, while those of k_r^{av} are similar. Therefore, the lower values of k_f^{av} of the mutant are the major origin of the observed destabilization in the mutant intermediates as compared to those of the wild-type protein. However, the formation of a protein disulfide bond can be regarded as occurring in two stages (*12a*, *18*); the first stage is the rapid equilibrium between the reduced protein and the mixed-disulfide intermediate with DTT^{ox}, and the second stage is the intramolecular disulfide formation to produce DTT^{red}. Therefore, the overall forward rate constant (k_f) can be expressed as the product of the equilibrium constant of the first reaction (K_{DTT}) and the rate constant (k_{intra}) for formation of the intramolecular disulfide bond. With statistical factors taken into account, we obtain the following equation:

$$k_f^{av} = K_{DTT} \cdot k_{intra}^{av} \quad (6)$$

According to Rothwarf and Scheraga (*12c*), the value of K_{DTT} for wild-type RNase A is 6.5×10^{-3} M^{-1}. Since the value of K_{DTT} should be similar in both the mutant and the wild-type protein, the decrease in k_f^{av} for the mutant can be attributed to the decrease in k_{intra}^{av}. Consequently, the observed destabilization in the mutant intermediates ($\Delta\Delta G^\circ = 0.32$ kcal/mol on average) originates predominantly from the decrease in the values of k_{intra}^{av} of the mutant. The values of k_{intra}^{av} for [C65S,C72S], [C65A,C72A], and wild-type RNase A in Table 2 reflect this approximate 2-fold difference.

The decrease in the values of k_{intra}^{av} of the mutant may arise from several discrete energetic factors. One of them is the difference in loop entropy between the mutant and wild-type proteins. Since the 65−72 disulfide bond in the wild-type protein is located in the middle of the polypeptide chain, the loss of this disulfide bond in the mutant increases the average length of possible disulfide loops for the mutant as compared to that for the wild-type protein. This effect increases the entropy loss of the mutant for formation of a disulfide bond and therefore destabilizes the disulfide-bonded forms of the regeneration intermediates of the mutant. In wild-type RNase A, the average entropy loss due to formation of all possible disulfide loops was calculated to be −16.80 eu, while in the mutant the corresponding value was −17.42 eu, by using the equation

$$\Delta S = -R[3.47 + 1.5 \ln(N)] \quad (7)$$

where ΔS is the entropy decrease due to formation of a disulfide bond, R is the gas constant, and N is the number of residues between the C^α atoms of the two cysteines (*22*, *38*). The energy difference corresponding to this loop entropy effect is 0.18 kcal/mol at 25 °C if disulfide-bond formation occurs completely randomly.

It is important to note that the proposed loop entropy effect of the mutation ($\Delta\Delta G^\circ < 0.18$ kcal/mol at 25 °C) is not sufficient to account for the observed destabilization ($\Delta\Delta G^\circ = 0.32$ kcal/mol) of the mutant intermediates; about half of the destabilization energy may arise from other energetic factors that decelerate the formation of intramolecular disulfide bonds (the k_{intra} process) for the mutant. Since these decelerating factors arise from the loss of Cys65 and Cys72 in the mutant and the 65−72 disulfide-bonded intermediate is a major component of the 1S ensemble for the wild-type protein (*22*), it is suggested that accelerating factors exist around the 65−72 disulfide loop for the regeneration of wild-type RNase A. One reasonable explanation is that the formation of the 65−72 disulfide bond accompanies the formation of enthalpically stable local structures near the 65−72 disulfide loop in the course of regeneration of wild-type RNase A, which facilitate formation of this disulfide bond and also subsequent ones.

By contrast, the values of k_r^{av} of [C65S,C72S] and wild-type RNase A were similar. They were also similar to each other within the same protein. Since the k_r process is a bimolecular reaction between the protein and DTT^{red}, the constant value of k_r^{av} means that any of the individual disulfide bonds in the intermediates has a similar chance to react with DTT^{red}. In other words, all disulfide bonds are exposed to the solvent to a similar extent. This strongly suggests that all preequilibrium intermediates of [C65S, C72S] are structurally disordered. This is in agreement with the previous conclusion by Rothwarf and Scheraga (*12b*) that the preequilibrium intermediates of RNase A are predominantly disordered.

Roles of Cys65 and Cys72 as a Chain Folding Initiation Site (CFIS). The 65−72 disulfide loop has been proposed as one of the chain folding initiation sites (CFIS) of RNase A (*21*). This region folds in the early stages of the regeneration and plays important roles in the subsequent folding events. Xu et al. (*22*) have recently shown that the one-disulfide intermediate that has the 65−72 disulfide linkage accumulates to the extent of 40% of all the possible 28 1S intermediates of RNase A. Further, the population of the 65−72 disulfide intermediate is significantly greater than that expected for a random distribution, as deduced from loop entropy calculations; therefore, there are interactions in the 65−72 disulfide loop, which stabilize the regeneration intermediates. These interactions may arise from the formation of the β-turn in the 65−72 disulfide loop (*22*).

The results of the kinetic analysis presented in this paper support the conclusion that the formation of the 65−72 disulfide loop accelerates the subsequent folding events; in the absence of the 65−72 disulfide loop, the folding of [C65S,C72S] RNase A was significantly slowed, as shown by the decrease in the values of k_{intra}^{av}. Moreover, this decrease possibly arises not only from the change of the loop entropy caused by the mutation but also from other energetic factors. Thus, it is likely that there are specific interactions around the region of the 65−72 disulfide loop, which accelerate the subsequent folding events. These interactions may draw other regions of the polypeptide chain close to the 65−72 disulfide loop so as to make the formation of the next disulfide bond easier. A recent NMR study of the [C65S,C72S] mutant (*19*) has indicated a conformational relationship between the 65−72 disulfide loop and the C-terminus. Thus, one candidate for the region that may be drawn close to the 65−72 loop consists of the β strands containing the hydrophobic core at the C-terminus.

Estimation of Disulfide Rearrangement Rates. Since k_{intra} is the rate constant for the intramolecular disulfide-bond formation process, it can serve as a good estimate for the rate of intramolecular disulfide rearrangement (reshuffling) (*12a*, *b*). Therefore, the expected value for the reshuffling rate constant from one to the other is $\sim$4 min^{-1} on average in the mutants. Provided that the concentration of DTT^{ox} and DTT^{red} is less than 200 and 0.1 mM, respectively, the rate of rearrangement is on average at least 2 orders of magnitude faster than those of the oxidation and reduction under the steady-state conditions. For example, the average rates of oxidation and reduction for 2S intermediates are calculated to be less than $2.2 \times 10^{-2} \times 0.2[2S] = 0.0044[2S]$ ($M \cdot min^{-1}$) and $4.7 \times 10^{2} \times 0.0001[2S] = 0.047[2S]$ ($M \cdot min^{-1}$), respectively, while the average rate of rearrangement is $\sim$4[2S] ($M \cdot min^{-1}$). This is the basis of our kinetic analysis in which all disulfide intermediates are treated as groups. It should be noted that the individual rate constants of the disulfide reshuffling can vary significantly depending on the length of the loop forming the disulfide bond. Other factors, such as the effect of local structures that resist the intramolecular nucleophilic attack of a free thiol, may also be involved.

Comparison with Other Three-Disulfide Proteins. Although the mutants examined here are not natural products, their regeneration can be considered as an example of the possible folding behavior of three-disulfide proteins. Some other proteins that have three-disulfide bonds have been studied, including BPTI (*39*, *40*), hirudin (*18*, *41*), tick anticoagulant peptide (*42*), ω-conotoxins (*43*), and [C40A, C95A] RNase A, another three-disulfide mutant of RNase A (*15*). Although the regeneration of BPTI is one of the most studied, only a limited number of disulfide intermediates have been observed; most of them have a conformation similar to that of the native protein. These properties made it easier to analyze the kinetics of folding of BPTI as compared to those of other proteins. However, from the general view of protein folding, they provided limited information about the local interresidue interactions that dictate the conformational folding of proteins. Recently, Dadlez and Kim (*44*) studied the early stages of the regeneration of BPTI from the totally reduced state by using recombinant variants of BPTI and found that the 14−38 disulfide bond, which is one of the three native disulfide bonds, forms much faster than any other possible single disulfide bond. This disulfide bond of BPTI may be regarded as an analogue of the 65−72 disulfide bond of RNase A. Very recently, Dadlez (*45*) reported that hydrophobic interactions accelerate the formation of the 14−38 disulfide bond in BPTI, while Xu et al. (*22*) have suggested that a β-turn stabilizes the formation of the 65−72 disulfide bond in RNase A.

On the other hand, the regeneration pathways of other three-disulfide proteins are generally more complicated. For example, in the regeneration of hirudin, many disulfide intermediates appear (*41*). By using DTT^{ox}/DTT^{red} as a redox couple and AEMTS as a thiol-blocking agent, Thannhauser et al. (*18*) have recently shown that the regeneration intermediates of hirudin attain a preequilibrium, as in [C65S, C72S] and [C65A,C72A], and that the major rate-determining step is the oxidation process from 2S to 3S*. Although this kinetic behavior is similar to those of [C65S,C72S] and [C65A,C72A], the average rate constants of forward and reverse reactions for hirudin decrease with formation and disruption, respectively, of disulfide bonds, whereas those for [C65S,C72S] and [C65A,C72A] do not. The difference may arise from the lower regeneration temperature (12 °C) used in the study of hirudin (*18*) or some other intrinsic factors residing in the amino acid sequence. The regeneration pathway of [C40A,C95A] RNase A has also been studied under similar regeneration conditions (*15*). It has been found that the regeneration intermediates of that mutant achieve a steady state, and the rate-determining step is the oxidation from 2S to 3S*. These properties are similar to those of [C65S/A,C72S/A] RNase A and hirudin, suggesting that achievement of a steady state between a number of

intermediates is a general phenomenon of disulfide-coupled regeneration of proteins.

As for the regeneration of other three-disulfide proteins, tick anticoagulant peptide (*42*) and ω-conotoxins (*43*), a number of disordered intermediates have been observed. These results as well as those for the regeneration pathways of hirudin (*18*) and the RNase A mutants (this work and ref 15) strongly suggest that the regeneration of three-disulfide proteins is generally complex with a number of internal disulfide-bonded intermediates (75 species as a maximum) being populated.

CONCLUSION

By using the [C65S,C72S] and [C65A,C72A] mutants, we characterized a minor regeneration pathway for wild-type RNase A in which the rate-determining step is the oxidation process from 2S to 3S* (des-[65−72]). This minor pathway could populate up to 3% under normal regeneration conditions. This finding reconfirms earlier conclusions (*7*, *12*, *17*) that the regeneration of RNase A follows multiple folding pathways. The complete kinetic analyses of the regeneration pathways for these mutants and the disulfide-loop entropy calculations have revealed the existence of decelerating factors for the regeneration of the mutants arising from the loss of the 65−72 disulfide loop. This in turn indicates that the regeneration of the wild-type protein is accelerated by formation of the 65−72 disulfide loop. The roles of Cys65 and Cys72 can be regarded as providing an entropic force and also an enthalpically stabilized small disulfide loop in the early stages of folding so as to facilitate the subsequent regeneration events.

ACKNOWLEDGMENT

We thank M. A. McDonald for preparing the recombinant plasmids to express the [C65S,C72S] and [C65A,C72A] RNase A mutants, and D. M. Rothwarf, Y. -J. Li, X. Xu, and T. W. Thannhauser for experimental assistance and many helpful discussions. M. Iwaoka thanks the Yamada Science Foundation (Osaka, Japan) for a research fellowship during his stay at Cornell University.

REFERENCES

1. Anfinsen, C. B. (1973) *Science 181*, 223.
2. Hantgen, R. R., Hammes, G. G., and Scheraga, H. A. (1974) *Biochemistry 13*, 3421.
3. Ahmed, A. K., Schaffer, S. W., and Wetlaufer, D. B. (1975) *J. Biol. Chem. 250*, 8477.
4. Takahashi, S., and Ooi, T. (1976) *Bull. Inst. Chem. Res., Kyoto Univ. 54*, 141.
5. (a) Creighton, T. E. (1977) *J. Mol. Biol. 113*, 275. (b) Creighton, T. E. (1977) *J. Mol. Biol. 113*, 329. (c) Creighton, T. E. (1979) *J. Mol. Biol. 129*, 411.
6. (a) Konishi, Y., and Scheraga, H. A. (1980) *Biochemistry 19*, 1308. (b) Konishi, Y., and Scheraga, H. A. (1980) *Biochemistry 19*, 1316.
7. (a) Konishi, Y., Ooi, T., and Scheraga, H. A. (1981) *Biochemistry 20*, 3945. (b) Konishi, Y., Ooi, T., and Scheraga, H. A. (1982) *Biochemistry 21*, 4734. (c) Konishi, Y., Ooi, T., and Scheraga, H. A. (1982) *Biochemistry 21*, 4741.
8. Wearne, S. J., and Creighton, T. E. (1988) *Proteins: Struct., Funct., Genet. 4*, 251.
9. Schultz, D. A., Schmid, F. X., and Baldwin, R. L. (1992) *Protein Sci. 1*, 917.
10. Ruoppolo, M., Torella, C., Kanda, F., Panico, M., Pucci, P., Marino, G., and Morris, H. R. (1996) *Folding Des. 1*, 381.
11. Rothwarf, D. M., and Scheraga, H. A. (1991) *J. Am. Chem. Soc. 113*, 6293.
12. (a) Rothwarf, D. M., and Scheraga, H. A. (1993) *Biochemistry 32*, 2671. (b) Rothwarf, D. M., and Scheraga, H. A. (1993) *Biochemistry 32*, 2680. (c) Rothwarf, D. M., and Scheraga, H. A. (1993) *Biochemistry 32*, 2690. (d) Rothwarf, D. M., and Scheraga, H. A. (1993) *Biochemistry 32*, 2698.
13. (a) Rothwarf, D. M., Li, Y.-J., and Scheraga, H. A. (1998) *Biochemistry 37*, 3760−3766. (b) Rothwarf, D. M., Li, Y.-J., and Scheraga, H. A. (1998) *Biochemistry 37*, 3767−3776.
14. Lester, C. C., Xu, X., Laity, J. H., Shimotakahara, S., and Scheraga, H. A. (1997) *Biochemistry, 36*, 13068.
15. Xu, X., and Scheraga, H. A. (1998) *Biochemistry*, submitted.
16. Creighton, T. E. (1988) *Proc. Natl. Acad. Sci. U.S.A. 85*, 5082.
17. (a) Scheraga, H. A., Konishi, Y., and Ooi, T. (1984) *Adv. Biophys. 18*, 21. (b) Scheraga, H. A., Konishi, Y., Rothwarf, D. M., and Mui, P. W. (1987) *Proc. Natl. Acad. Sci. U.S.A. 84*, 5740.
18. Thannhauser, T. W., Rothwarf, D. M., and Scheraga, H. A. (1997) *Biochemistry 36*, 2154.
19. Shimotakahara, S., Rios, C. B., Laity, J. H., Zimmerman, D. E., Scheraga, H. A., and Montelione, G. T. (1997) *Biochemistry 36*, 6915.
20. Laity, J. H., Lester, C. C., Shimotakahara, S., Zimmerman, D. E., Montelione, G. T., and Scheraga, H. A. (1997) *Biochemistry 36*, 12683−12699.
21. (a) Némethy, G., and Scheraga, H. A. (1979) *Proc. Natl. Acad. Sci. U.S.A. 76*, 6050. (b) Montelione, G. T., and Scheraga, H. A. (1989) *Acc. Chem. Res. 22*, 70.
22. Xu, X., Rothwarf, D. M., and Scheraga, H. A. (1996) *Biochemistry 35*, 6406.
23. (a) Wetlaufer, D. B. (1973) *Proc. Natl. Acad. Sci. U.S.A. 70*, 697. (b) Matheson, R. R., Jr., and Scheraga, H. A. (1978) *Macromolecules 11*, 819. (c) Baldwin, R. L. (1989) *Trends Biochem. Sci. 14*, 291. (d) Freund, S. M. V., Wong, K.-B., and Fersht, A. R. (1996) *Proc. Natl. Acad. Sci. U.S.A. 93*, 10600.
24. Ellman, G. L. (1959) *Arch. Biochem. Biophys. 82*, 70.
25. Thannhauser, T. W., Konishi, Y., and Scheraga, H. A. (1984) *Anal. Biochem. 138*, 181.
26. Bruice, T. W., and Kenyon, G. L. (1982) *J. Protein Chem. 1*, 47.
27. Laity, J. H., Shimotakahara, S., and Scheraga, H. A. (1993) *Proc. Natl. Acad. Sci. U.S.A. 90*, 615.
28. delCardayré, S. B., Ribó, M., Yokel, E. M., Quirk, D. J., Rutter, W. J., and Raines, R. T. (1995) *Protein Eng. 8*, 261.
29. Thannhauser, T. W., McWherter, C. A., and Scheraga, H. A. (1985) *Anal. Biochem. 149*, 322.
30. Beavis, R. C., and Chait, B. T. (1989) *Rapid Commun. Mass Spectrom. 3*, 233.
31. Li, Y.-J., Rothwarf, D. M., and Scheraga, H. A. (1995) *Nature Struct. Biol. 2*, 489.
32. Straume, M., and Johnson, M. L. (1992) *Methods Enzymol. 210*, 117.
33. Meinwald, Y. C., Stimson, E. R., and Scheraga, H. A. (1986) *Int. J. Peptide Protein Res. 28*, 79.
34. van Mierlo, C. P. M., Darby, N. J., Neuhaus, D., and Creighton, T. E. (1991) *J. Mol. Biol. 222*, 373.
35. Staley, J. P., and Kim, P. S. (1992) *Proc. Natl. Acad. Sci. U.S.A. 89*, 1519.
36. Liu, Y., Breslauer, K., and Anderson, S. (1997) *Biochemistry 36*, 5323.

37. Talluri, S., Rothwarf, D. M., and Scheraga, H. A. (1994) *Biochemistry 33*, 10437.
38. Lin, S. H., Konishi, Y., Denton, M. E., and Scheraga, H. A. (1984) *Biochemistry 23*, 5504.
39. (a) Creighton, T. E. (1978) *Prog. Biophys. Mol. Biol. 33*, 231. (b) Creighton, T. E., and Goldenberg, D. P. (1984) *J. Mol. Biol. 179*, 497. (c) Creighton, T. E. (1990) *Biochem. J. 270*, 1. (d) Creighton, T. E. (1992) *Science 256*, 111.
40. Weissman, J. S., and Kim, P. S. (1991) *Science 253*, 1386.
41. (a) Chatrenet, B., and Chang, J.-Y. (1992) *J. Biol. Chem. 267*, 3038. (b) Chatrenet, B., and Chang, J.-Y. (1993) *J. Biol. Chem. 268*, 20988.
42. Chang, J.-Y. (1996) *Biochemistry 35*, 11702.
43. Price-Carter, M., Gray, W. R., and Goldenberg, D. P. (1996) *Biochemistry 35*, 15537.
44. Dadlez, M., and Kim, P. S. (1996) *Biochemistry 35*, 16153.
45. Dadlez, M. (1997) *Biochemistry 36*, 2788.

BI9725327